Frustrated Spin Model as a Hard-Sphere Liquid

Frustrated spin model as a hard-sphere liquid

M. V. Mostovoy, D. I. Khomskii, and J. Knoester
Materials Science Center, University of Groningen, Nijenborgh 4, 9747 AG Groningen, The Netherlands

N. V. Prokof'ev
Physics and Astronomy, Hasbrouck Laboratory, University of Massachusetts, Amherst, MA 01003, USA

(Dated: February 1, 2008)

We show that one-dimensional topological objects (kinks) are natural degrees of freedom for an antiferromagnetic Ising model on a triangular lattice. Its ground states and the coexistence of spin ordering with an extensive zero-temperature entropy can be easily understood in terms of kinks forming a hard-sphere liquid. Using this picture we explain effects of quantum spin dynamics on that frustrated model, which we also study numerically.

PACS numbers: 05.50.+q, 75.10.Jm, 75.30.Fv, 64.60.Cn

Geometrically frustrated materials recently emerged as a new broad class of solids with interesting and rather unusual properties [1]. While some of these systems stay disordered at all temperatures, others order often in an unexpected way, showing no universality typical for critical behavior of conventional systems. One may wonder, however, to which extent the complexity of ground states and excitations of frustrated models is their genuine property and to which it is, essentially, a conventional behavior obscured by an unfortunate choice of variables, in which these models are formulated. In this Letter we consider a frustrated Ising model showing a spin-density-wave (SDW) ordering, more common for systems with continuous symmetries. We explain the origin of this strange behavior and give a simple description of ground states of that model (the number of which grows exponentially with the system size) by mapping it on a hard-sphere liquid. We use this approach to study the role of quantum spin fluctuations, which for frustrated systems is a challenging theoretical problem [2, 3]. We also show that the low-energy states of our model form a large number of valleys separated by energy barriers, which prevents the system from reaching thermal equilibrium at low temperatures, but does not result in a spin-glass behavior in the absence of quenched disorder [4, 5].

One of the simplest classical frustrated models describes the Ising spins $\sigma_i = \pm 1$ on sites of a triangular lattice with nearest-neighbor antiferromagnetic interactions:

$$E = J \sum_{\langle i,j \rangle} \sigma_i \sigma_j, \quad J > 0. \tag{1}$$

This system stays disordered at all nonzero temperatures [6, 7], while at $T = 0$ the spins order periodically

$$\langle \sigma_i \sigma_j \rangle \propto \frac{1}{r_{ij}^{\eta}} \cos \frac{2\pi r_{ij}}{3}, \tag{2}$$

where r_{ij} is the distance between the spins and $\eta = 1/2$ [8]. This algebraic order coexists with an extensive zero temperature entropy $S_0 \approx 0.323 k_B$ per spin [6, 7].

This entropically induced ordering resembles the crystallization in hard-sphere liquids at high volume fractions [9, 10]. We show below that the model Eq.(1) can indeed be mapped on a two-dimensional liquid of topological domain walls (kinks), the motion of which is confined to one spatial dimension. This mapping also provides useful insights into the physics of the quantum version of Eq.(1)

$$H = J \sum_{\langle i,j \rangle} \sigma_i^z \sigma_j^z - h \sum_i \sigma_i^x, \tag{3}$$

where $\sigma_i^{x,z}$ are the Pauli matrices and h is the transverse field (the classical and quantum frustrated models Eq.(1) and Eq.(3) are referred to below as, respectively, CFM and QFM). The critical behavior in the QFM was recently discussed by Moessner *et al.*, who argued that the ordering of quantum spins is long-ranged at low temperatures and that the ordered and disordered phases are separated by a phase with algebraically decaying spin correlations [11, 12]. Here we show that the difference in the critical behavior of the CFM and QFM originates from a higher rigidity of the quantum kink crystal. We also perform numerical simulations of the QFM and find an unexpected specific heat anomaly at strong transverse fields.

Kinks in frustrated Ising model: We shall consider the triangular lattice as an array of coupled chains, running in the x-direction. As neighboring chains are shifted with respect to each other, we will distinguish even and odd chains. In each chain we perform the transformation from spins to kinks, which are domain walls separating two different Neel states and carrying the topological charge $q = \pm 1$ (kinks and antikinks). The chain energy equals $2JN$, where N is the number of kinks, independent of kink positions. The interchain spin coupling gives rise to interactions between pairs of kinks in neighboring chains with the potential

$$V(x_o - x_e) = 2J q_o q_e \mathrm{sign}(x_o - x_e), \tag{4}$$

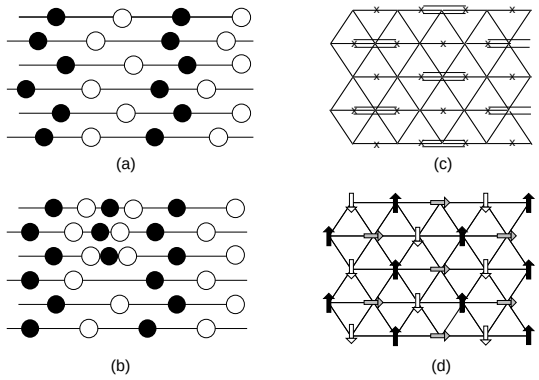

FIG. 1: (a) Optimal relative ordering of kinks; the black(white) circles correspond to kinks with the topological charge $+1(-1)$; (b) Dislocation in the kink crystal with the energy $2J$;(c) The kink crystal, in which the kinks delocalized over pairs of neighboring sites are indicated by dimers; (d) The spin ordering corresponding to the kink crystal.

where $q_o(q_e)$ and $x_o(x_e)$ are, respectively, the topological charges and x-coordinates of the kinks in the odd(even) chain. This potential only depends on the sign of the relative coordinate $x_o - x_e$. Therefore, the energy of the CFM is completely determined by the number of kinks and their relative ordering in neighboring chains. These loose interactions between kinks are much different from those in unfrustrated models (e.g., the Ising model on a square lattice) which grow linearly with the distance between kinks, confining them into pairs.

While in unfrustrated models the density of kinks vanishes at low temperatures, in the CFM kinks are present in ground states. In the energetically most favorable relative ordering the $q = +1$ kink in an odd chain has the nearest-neighbor $q = +1(-1)$ kinks in two neighboring even chains from the right/left and vice versa (see Fig. 1a), in which case the kink creation energy $2J$ is exactly compensated by the energy of its interactions with kinks in neighboring chains, i.e. in the ground states kinks cost no energy. For the favorable relative ordering the number of kinks N in each chain has to be the same. Therefore, the ground states form distinct classes labeled by N. Since shifts of kinks that preserve the ordering do not change energy, each class still contains a large number of states, resulting in an extensive ground state entropy.

To describe the statistics of kinks in the ground state class N, we introduce the 'wave function' $\Psi_N\{z\}$, which equals the number of the minimal-energy kink configurations in the lower half-plane for fixed positions of the N kinks in the uppermost chain represented by $\{z\} = (z_1, z_2, \ldots, z_N)$, where $z_j = e^{2\pi i \frac{x_j}{L_x}}$ and L_x is the chain length. One can then add one more chain from above and obtain an eigenvalue equation for the wave function

$$\lambda_N \Psi_N\{z\} = {\sum_{\{z'\}}}' \Psi_N\{z'\}, \tag{5}$$

where the ${\sum}'$ denotes the summation that preserves the energetically favorable relative ordering of kinks with the coordinates $\{z\}$ and $\{z'\}$ in two neighboring chains. The solution of Eq.(5) is the absolute value of the van der Monde determinant

$$\Psi_N(z_1, z_2, \ldots, z_N) \propto \prod_{i<j} |z_i - z_j|, \tag{6}$$

It can also be written in the form of the Slater determinant of N plane waves $e^{ik_n x_j}$ $(n, j = 1, 2, \ldots, N)$ with the wave vectors k_n taking values in the Fermi sea $-k_F < k < +k_F$, where the Fermi wave vector k_F is related to the density of kinks $n = \frac{N}{L_x}$ by $k_F = \pi n$. Thus, Eq.(6) is the ground-state wave function of N fermions in the chain with L_x sites and the kinks can be identified with the fermions appearing in the transfer-matrix solution of the CFM [13].

The eigenvalue λ_N in Eq.(5) is related to the number of the ground states in this class, W_N, by $W_N = \lambda_N^{L_y}$ (L_y is the number of chains). In the limit $L_x, L_y \to \infty$ and for a fixed kink density n, $\lambda_N \sim e^{L_x S(n)} \frac{2\pi}{\sqrt{L_x \tan \frac{\pi n}{2}}}$, where $S(n)$ is the ground-state entropy per site

$$S(n) = \frac{1}{\pi} \int_0^{\pi n} d\phi \ln \left(2 \cos \frac{\phi}{2} \right). \tag{7}$$

For $n = \frac{1}{3}$, at which $S(n)$ has its maximum, Eq.(7) gives the value $\sim 0.323 k_B$ cited above.

The joint distribution function $P_N(\{z\})$ of N kinks in a chain is obtained by summing over all minimal-energy configurations of kinks in the chains *both below and above* this chain, which gives

$$P_N\{z\} = \Psi_N^2\{z\} \propto \prod_{i<j} |z_i - z_j|^2. \tag{8}$$

The spin correlation function along chains $\langle \sigma_x \sigma_0 \rangle = (-)^x \langle (-)^{K(x)} \rangle$, where $K(x)$ is the number of the kinks in the interval $[0, x]$. Using Eq.(8), the spin correlator can be written in the form of the Toeplitz determinant: $\langle \sigma_x \sigma_0 \rangle = (-)^x \det f_{nm}$, where $f_{nm} = \delta_{nm} - \frac{2}{L_x} \frac{\sin \frac{\pi(n-m)x}{L_x}}{\sin \frac{\pi(n-m)}{L_x}}$. For $1 \ll x \ll L_x$, the determinant $\propto \frac{1}{\sqrt{x}} \cos k_F x$, so that for $k_F = \frac{\pi}{3}$ we recover Eq.(2). In general, the ground state class with N kinks/chain has an algebraic SDW order with the wave vector $q = \pi(1 - n)$, which we interpret as the $2k_F$-instability of the kink Fermi sea. For Ising-type models with the discrete Z_2 symmetry such SDW states are very unusual.

The number of ground states W_N has a sharp peak at $N_* = L_x/3$: $W_N \propto \exp\left[-\text{const} \frac{L_y}{L_x} (N - N_*)^2 \right]$. Though the number of classes significantly contributing to the CFM partition function stays finite in the thermodynamic limit, all of them are essentially identical copies of the class with $n = 1/3$, since the corresponding SDW

vectors deviate from $q = 2\pi/3$ by an amount $\propto 1/L_x$. Furthermore, the deviation of the total ground state entropy per spin $S = \frac{1}{L}\ln\sum_N W_N$, where $L = L_xL_y$ is the number of spins, from the entropy of a single class Eq.(7) at $n = \frac{1}{3}$ is $O(1/L)$. Thus, in the thermodynamic limit it suffices to consider only one class with 1 kink per 3 sites. *Quantum model:* The transverse field h in Eq.(3) flips spins, resulting in hopping of kinks along the chains, as well as in creation/annihilation of kink-antikink pairs on neighboring chain sites. For $h \ll J$ the hopping plays the dominant role, as it mixes degenerate classical ground states within each class, whereas the kink-antikink pairs cost energy $\sim 4J$ and only appear virtually, renormalizing the kink dispersion: $E(k) \approx -2h\cos k + \frac{h^2}{J}\left(\sin^2 k + \frac{1}{6}\right)$. Here k is the kink wave vector, the first term is due to the hopping of kinks on neighboring sites, and the second term contains contributions from the dressing of kinks and the ground state by one virtual kink-antikink pair. For $h, T \ll J$ the positions of the dressed kinks satisfy the same restrictions as in the classical ground states and h is the only relevant energy scale. In other words, kinks form a quantum hard sphere liquid. The restricted motion of kinks makes the quantum system more rigid than the classical one and gives rise to phonon-like excitations with velocity $\propto h$.

In the CFM kinks only crystallize at $T = 0$. At any nonzero temperature the algebraic order is destroyed by dislocations in the kink crystal with energy $2J$ (see Fig.1b), which in the classical model are unbound. The latter leads to the asymptotic behavior of the spin correlation function at $T \ll J$ [8], given by the right-hand side of Eq.(2) multiplied by $e^{-r_{ij}/\xi}$, where $\xi = e^{2\beta J}$ is the average distance between the dislocations. On the other hand, in the QFM phonons result in two-dimensional Coulomb interactions $U(r) \propto h\ln r$ between the dislocations separated by a distance r, binding them into pairs at a finite temperature $T_1 \propto h$, below which the spin correlations decay algebraically [14]. Upon lowering temperature, the exponent η (see Eq.(2)) decreases, as the kink crystal becomes more rigid, which ultimately leads to the pinning of the kink crystal by the lattice at some temperature $T_2 < T_1$, below which the phonons become gapped and the spin ordering becomes long-ranged [15, 16, 17]. A cartoon of the quantum kink crystal with 1 kink per 3 sites is shown in Fig.1c. To gain kinetic energy each kink is delocalized over one bond (such bonds are shown as dimers) and the bonds are arranged in a way that ensures the energetically favorable ordering of kinks. This state corresponds to the SDW state with the wave vector $q = \frac{2\pi}{3}$ (see Fig. 1d), in which the spins antiferromagnetically ordered along the z axis form a bipartite hexagonal lattice, while the spins located in the centers of the hexagons are oriented along the transverse field, since the fields from their neighbors add to zero.

Thus for weak transverse fields $h \ll J$, the QFM describes a kink crystal that melts like a crystal of adsorption atoms on a substrate lattice, i.e. the melting is preceded by a depinning transition and the solid phase is separated from the liquid phase by a 'floating crystal phase' with algebraic crystal order [15, 16, 17]. In the context of the QFM this phase diagram was recently suggested by Moessner et al. [11, 12], who studied the critical behavior of the QFM in the vicinity the quantum critical point, i.e. in the opposite limit of strong transverse fields $h \sim J$. Two-dimensional crystals are also known to melt via a single first-order transition due to proliferation of the boundaries between degenerate crystal phases [10, 17, 18]. We compare these two scenarios to our numerical results.

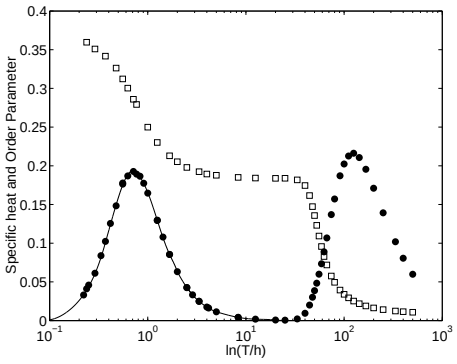

FIG. 2: The plot of specific heat (circles) and the 'order parameter' m (squares) of the QFM vs h/T, for $h \ll J$. The smooth line interpolates the part of $c(h/T)$ due to quantum superpositions of classical ground states.

Numerical results: We performed Monte Carlo simulations of the QFM using the continuous time algorithm [19], calculating the temperature dependence of the specific heat c and the susceptibilities $\chi_q = \langle M_q^2\rangle/L$, where $M_q = \sum_j \sigma_j^z \cos qx_j$ and q is a multiple of $\frac{2\pi}{L_x}$. A large value of χ_q is a signature of the SDW state with the wave vector q. We also calculate the finite system 'order parameter' $m = \sqrt{\langle M_{2\pi/3}^2\rangle}/L$.

The behavior of the model is most spectacular for weak transverse fields, $h \ll J = 1$, when one can see a clear difference between the classical and quantum regimes. In Fig.2 we plot the specific heat and 'order parameter' as a function of the ratio T/h, varying over four decades and covering both the classical region $h \ll T, J$ and the quantum region $h, T \ll J$. The 'classical points' are calculated at $h = 0.01$, while the 'quantum data' is a collection for many (h, T) points, which fall on smooth curves when plotted versus T/h, showing that in the quantum regime h is indeed the only relevant energy scale. The specific heat has two maxima: one at $T \sim J$, which also exists in the classical model, and another at $T \sim h$, due to quantum superpositions of classical ground states. To show that the huge degeneracy of the classical model is lifted by a transverse field, we calculate the entropy release

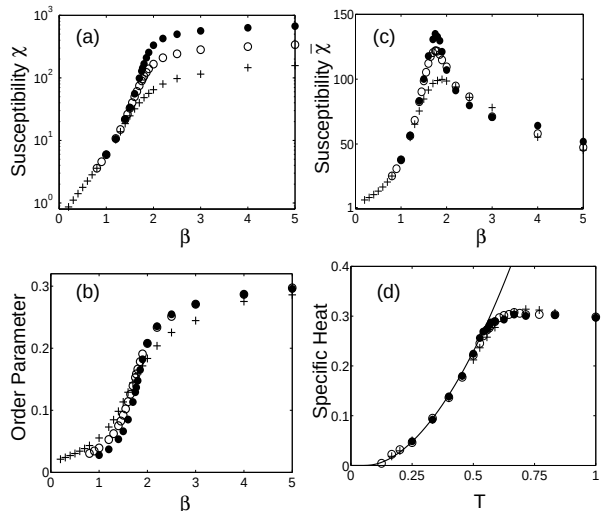

FIG. 3: The susceptibility χ (a), the 'order parameter' m (b), and the susceptibility $\bar{\chi}$ (c) versus inverse temperature β for $h = J = 1$, $L_x = 96$ and three different values of L_y: 20 (pluses), 40 (open circles), and 80 (filled circles). Plotted in panel (d) is the corresponding temperature dependence of the specific heat. The solid line is the specific heat of two-dimensional phonons with a gap ~ 0.5.

related to the low-T maximum, $\Delta S = \int_0^{T_*} \frac{dT}{T} c$, where $h \ll T_* \ll J$. The numerical integration that uses the smooth-curve fit of the MC data (see Fig.2) gives $\Delta S = 0.32 k_B$, in perfect agreement with the zero temperature entropy of the classical model. The 'classical maximum' corresponds to the disappearance of defects in the kink crystal with the energy $\sim J$, which *in finite systems* induces an algebraic spin ordering with $\eta = \frac{1}{2}$, just as in the CFM at $T = 0$. The latter is clear from the temperature dependence of the 'order parameter', which grows fast at $T \sim J$ and stays constant at $h \ll T \ll J$. At $T \sim h$, the 'order parameter' grows again, reflecting the increasing stiffness of the kink crystal due to the quantum motion of kinks, which results in a decrease of the exponent η and, perhaps, in the appearance of the long-range order. The smooth temperature dependence of c and m is evidence against a first-order transition and is compatible with the two phase-transitions scenario, since both transitions are expected to be of the Kosterlitz-Thouless type [16]. Furthermore, in a finite system the transition at the upper critical temperature $T_1 \sim h \ll J$, describing the dislocation binding does not occur, as all dislocations disappear at much higher temperature $\sim J$. The lower critical transition is also rather difficult to identify, since the algebraic order with $\eta = 1/9$ at $T = T_2 + 0$ [16] is practically indistinguishable from the long-range order at $T < T_2$.

In Figs. 3(a) and (b) we plot $\chi \equiv \chi_{2\pi/3}$ and m vs temperature, for the strong transverse field $h = J = 1$, $L_x = 96$, and $L_y = 20, 40$, and 80. For $\beta < 1.5$, the susceptibility/spin χ is independent of L_y, corresponding to a disordered phase, while for $\beta > 2$, the 'order parameter' m shows little size-dependence for large L_y, indicating a long-range ordering. On the basis of our data it is difficult to conclude whether the intermediate region $1.5 < \beta < 2$ is the 'algebraic' phase with temperature-dependent η or it is a vicinity of a single transition. Note, that the specific heat has a rather sharp kink at $\beta \sim 1.8$, at which its behavior changes from approximately temperature-independent to T^2-dependence, corresponding to the specific heat of phonons in the two-dimensional kink crystal (see Fig. 3(d)). Also the susceptibility $\bar{\chi} = \sum_{q \neq 2\pi/3} \chi_q$, describing SDWs with subdominant harmonics has a peak at $\beta = 1.75$ (see Fig. 3(c)), suggesting a single transition, which may be attributed to a sudden loss of rigidity of the kink crystal.

Topological spin glass?: We found that for $\beta J > 2$ it is effectively impossible to bring a large system into thermal equilibrium, as it 'freezes' in one of the SDW states with $q \sim 2\pi/3$. This 'glassy' behavior is related to the existence of different ground state classes, which in the quantum case transform into an array of energy valleys separated by barriers. At low T the barriers become impenetrable, as the tunneling between neighboring classes requires creating/annihilating a kink-antikink pair in all chains. Does such an energy landscape lead to a spin-glass behavior in the absence of quenched disorder and should the 'kink' in $c(T)$ at $T \sim 0.6$ (see Fig. 3c) be interpreted as a spin-glass transition? We believe that the answer is negative, because (as in the CFM) the number of important energy minima in the thermodynamics limit stays finite, all of them describing essentially the same state. In our low-T simulations we select the state with $q = 2\pi/3$ by an appropriate initial spin configuration.

In conclusion, we explained unusual properties of the classical and quantum frustrated Ising models by mapping them on a system of kinks, which behave like hard spheres. We showed that the quantum spin dynamics makes the kink crystal more rigid, resulting in a long range ordering at low temperatures. We studied numerically the temperature dependence of specific heat and spin susceptibility in weak and strong transverse fields.

This work is supported by the MSC^{plus} program and the NSF grant DMR 0071767. We thank R. Moessner and A. Tsvelik for useful discussions.

[1] For reviews, see P. Schiffer and A. P. Ramirez, Comments. Condens. Matter Phys. **18**, 21 (1996).
[2] C. Waldtmann *et al.*, Eur. Phys. J. B **2**, 501 (1998).
[3] B. Canals and C. Lacroix, Phys. Rev. Lett. **80**, 2933 (1998).
[4] G. Aeppli and P. Chandra, Science **275**, 177 (1997).
[5] J.S. Gardner *et al.* Phys. Rev. Lett. **83**, 211 (1999).
[6] G.H. Wannier, Phys. Rev. **79**, 357 (1950).
[7] R.M.F. Houtappel, Physica **16**, 425 (1950).
[8] J. Stephenson, J. Math. Phys. **11**, 413 (1970); *ibid* 420

(1970).
[9] B.J. Alder and T.E. Wainwright, Phys. Rev. **127**, 359 (1962).
[10] H. Weber, D. Marx, and K. Binder, Phys. Rev. B **51**, 14 636 (1995).
[11] R. Moessner, S.L. Sondhi, and P. Chandra, Phys. Rev. Lett. **84**, 4457 (2000).
[12] R. Moessner and S.L. Sondhi, Phys. Rev. B **63**, 224401 (2001).
[13] I. Peschel and V. J. Emery, Z. Phys. B **43**, 241 (1981).
[14] J. M. Kosterlitz and D. J. Thouless, J. Phys. C **6**, 1181 (1203).
[15] V. L. Pokrovsky and G. V. Umin, Zh. Eksp. Teor. Fiz. **65**, 1691 (1973).
[16] J.V. Jose, L.P. Kadanoff, S. Kirkpatrick, and D. R. Nelson, Phys. Rev. B **16**, 1217 (1977).
[17] B. I. Halperin and D. R. Nelson, Phys. Rev. Lett. **41**, 121 (1978).
[18] S. T. Chui, Phys. Rev. Lett. **48**, 933 (1982).
[19] N.V. Prokof'ev, B.V. Svistunov, and I.S. Tupitsyn, Zh. Eksp. Teor. Fiz., **114**, 570 [Sov. Phys. JETP **87**, 310] (1998); Phys. Lett. A **238**, 253 (1998).